

Low temperature specific heat of superconducting ternary intermetallics  $\text{La}_3\text{Pd}_4\text{Ge}_4$ ,  $\text{La}_3\text{Ni}_4\text{Si}_4$ , and  $\text{La}_3\text{Ni}_4\text{Ge}_4$  with  $\text{U}_3\text{Ni}_4\text{Si}_4$ -type structure

This article has been downloaded from IOPscience. Please scroll down to see the full text article.

2008 J. Phys.: Condens. Matter 20 385204

(<http://iopscience.iop.org/0953-8984/20/38/385204>)

View [the table of contents for this issue](#), or go to the [journal homepage](#) for more

Download details:

IP Address: 129.252.86.83

The article was downloaded on 29/05/2010 at 15:07

Please note that [terms and conditions apply](#).

# Low temperature specific heat of superconducting ternary intermetallics $\text{La}_3\text{Pd}_4\text{Ge}_4$ , $\text{La}_3\text{Ni}_4\text{Si}_4$ , and $\text{La}_3\text{Ni}_4\text{Ge}_4$ with $\text{U}_3\text{Ni}_4\text{Si}_4$ -type structure

S Kasahara, H Fujii, H Takeya, T Mochiku, A D Thakur and K Hirata

Superconducting Materials Center, National Institute for Materials Science, 1-2-1 Sengen, Tsukuba, Ibaraki 305-0047, Japan

E-mail: [Kasahara.Shigeru@nims.go.jp](mailto:Kasahara.Shigeru@nims.go.jp)

Received 24 April 2008, in final form 1 August 2008

Published 21 August 2008

Online at [stacks.iop.org/JPhysCM/20/385204](http://stacks.iop.org/JPhysCM/20/385204)

## Abstract

A systematic investigation on the thermodynamic properties of La-based ternary intermetallic superconductors crystallizing in a  $\text{U}_3\text{Ni}_4\text{Si}_4$ -type structure is presented. The  $\text{U}_3\text{Ni}_4\text{Si}_4$ -type structure consists of a characteristic intergrowth of periodic  $\text{BaAl}_4$  ( $\text{ThCr}_2\text{Si}_2$ )- and  $\text{AlB}_2$ -type segments. Pristine low temperature specific heat data for recently discovered members  $\text{La}_3\text{Ni}_4\text{Si}_4$  and  $\text{La}_3\text{Ni}_4\text{Ge}_4$  with  $T_c$ s of 1.0 and 0.7 K, respectively, are presented as well as  $\text{La}_3\text{Pd}_4\text{Ge}_4$  with the highest  $T_c$  of 2.5 K in the  $\text{U}_3\text{Ni}_4\text{Si}_4$ -type group. Owing to the higher  $T_c$ s of  $\text{U}_3\text{Ni}_4\text{Si}_4$ -type superconductors than the related  $\text{ThCr}_2\text{Si}_2$ -type compounds, comparisons are drawn in our investigations of the ternary intermetallics of  $\text{LaPd}_2\text{Ge}_2$ ,  $\text{LaNi}_2\text{Si}_2$ , and  $\text{LaNi}_2\text{Ge}_2$  having a  $\text{ThCr}_2\text{Si}_2$ -type structure. Our investigations of the thermodynamic properties show that  $\text{La}_3\text{Ni}_4\text{Si}_4$  and  $\text{La}_3\text{Ni}_4\text{Ge}_4$  have higher values of  $\gamma_n$ ,  $N(E_F)$ , and  $\Theta_D$  than  $\text{La}_3\text{Pd}_4\text{Ge}_4$ . The same trend was found in  $\text{ThCr}_2\text{Si}_2$ -type compounds of  $\text{LaPd}_2\text{Ge}_2$ ,  $\text{LaNi}_2\text{Si}_2$ , and  $\text{LaNi}_2\text{Ge}_2$ . It turns out that the difference in  $T_c$  between  $\text{La}_3\text{Pd}_4\text{Ge}_4$ ,  $\text{La}_3\text{Ni}_4\text{Si}_4$ , and  $\text{La}_3\text{Ni}_4\text{Ge}_4$ , as well as the relatively higher  $T_c$  of the  $\text{U}_3\text{Ni}_4\text{Si}_4$ -type superconductors than of the related  $\text{ThCr}_2\text{Si}_2$ -type compounds, are largely due to the strength of electron–phonon coupling.

(Some figures in this article are in colour only in the electronic version)

## 1. Introduction

Ternary intermetallics with a  $\text{ThCr}_2\text{Si}_2$ -type structure [1, 2], a  $\text{BaAl}_4$  derivative, have been studied extensively—especially the issues related to superconductivity and magnetism. A number of compounds crystallize with rare-earth ions, in which the 4f (or 5f) electrons hybridize with the conduction electrons and often provide exotic properties. For instance,  $\text{CeCu}_2\text{Si}_2$  is the first superconducting material with heavy fermion properties [3]. Compounds crystallizing in the  $\text{ThCr}_2\text{Si}_2$ -type structure show a rich variety of phenomena related to superconductivity. However, the superconducting critical temperature ( $T_c$ ) in most of such compounds is as low as 1 K, as found for  $\text{LaPd}_2\text{Ge}_2$  and  $\text{LaPt}_2\text{Ge}_2$  with  $T_c$ s of 1.12 and

0.55 K [4]<sup>1</sup>. Meanwhile, significant interest is being generated by the existence of further derivative structures. Among the  $\text{ThCr}_2\text{Si}_2$ -based derivatives, quaternary intermetallic borocarbides have a derivative structure, interstitially filled by carbon atoms. As represented by the 23 K superconductivity in  $\text{YPd}_2\text{B}_2\text{C}$ , which is the highest found in the  $\text{ThCr}_2\text{Si}_2$ -type derivatives (see footnote 1), some borocarbides undergo a superconducting transition at moderately high  $T_c$ , and some of them show unconventional superconductivity [5–9].

Over the past several decades, investigations on various kinds of  $\text{ThCr}_2\text{Si}_2$ -derivatives have opened up new areas for

<sup>1</sup> During the reviewing process, the record of  $T_c$  in  $\text{ThCr}_2\text{Si}_2$ -type intermetallics was broken by the discovery of FeAs-based superconducting materials.

research on superconducting materials. The  $U_3Ni_4Si_4$ -type structure is also classified in the  $ThCr_2Si_2$  derivatives with a characteristic periodic intergrowth of  $BaAl_4$  ( $ThCr_2Si_2$ )- and  $AIB_2$ -type segments [10]. At present, only about 10 compounds have been found to be ternary  $U_3Ni_4Si_4$ -type materials [10–21]. Among them, superconductivity has been shown to exist in  $La_3Pd_4Ge_4$  and  $La_3Pd_4Si_4$  [19, 21]. The  $T_c$ s of  $La_3Pd_4Ge_4$  and  $La_3Pd_4Si_4$  (defined by the onset of diamagnetism) are 2.75 and 2.15 K, respectively. In addition, we have recently found superconductivity in two isostructural compounds,  $La_3Ni_4Si_4$  and  $La_3Ni_4Ge_4$ , with  $T_c$ s of 1.0 and 0.7 K, respectively [22].

Although, the above four compounds having the  $U_3Ni_4Si_4$ -type structure are found to undergo superconductivity, their detailed thermodynamic properties, as well as the coupling between electrons and phonons, have not been clarified yet. In this work we present the results from our investigations on low temperature specific heat in the  $U_3Ni_4Si_4$ -type superconductors  $La_3Pd_4Ge_4$ ,  $La_3Ni_4Si_4$ , and  $La_3Ni_4Ge_4$ . A related  $ThCr_2Si_2$ -type superconductor,  $LaPd_2Ge_2$  [4], and non-superconducting  $LaNi_2Si_2$ ,  $LaNi_2Ge_2$ , which are the segments of the  $U_3Ni_4Si_4$ -type compounds [10], are also studied. The Sommerfeld coefficient,  $\gamma_n$ , and the Debye temperature,  $\Theta_D$ , are obtained from the normal state specific heat. Based on the results, the electron–phonon coupling constant,  $\lambda_{ph}$ , and the electronic density of states at the Fermi level,  $N(E_F)$ , are derived for each compound. Our investigations into the thermodynamic properties show that  $La_3Ni_4Si_4$  and  $La_3Ni_4Ge_4$  have the higher values in  $\gamma_n$ ,  $N(E_F)$ , and  $\Theta_D$  than  $La_3Pd_4Ge_4$ . The same trend was found in the related  $ThCr_2Si_2$ -type compounds of  $LaPd_2Ge_2$ ,  $LaNi_2Si_2$ , and  $LaNi_2Ge_2$ . It turns out that the differences in  $T_c$  between  $La_3Pd_4Ge_4$ ,  $La_3Ni_4Si_4$ , and  $La_3Ni_4Ge_4$  are largely due to the strength of the electron–phonon coupling, while  $\Theta_D$  and  $N(E_F)$  have less weight on the superconductivity. It is also shown that all the La-based superconductors crystallize in the  $U_3Ni_4Si_4$ -type structure have higher  $\lambda_{ph}$  than the related  $ThCr_2Si_2$ -type compounds. The superconducting gap in each compound is discussed based on the electronic specific heat,  $C_{el}$ , in the superconducting state. We depict a systematic investigation of the thermodynamic and the superconducting properties in the  $U_3Ni_4Si_4$ - and the related  $ThCr_2Si_2$ -type compounds.

## 2. Experimental details

We synthesized  $La_3Pd_4Ge_4$ ,  $La_3Pd_4Si_4$ ,  $La_3Ni_4Si_4$ , and  $La_3Ni_4Ge_4$  by the standard arc-melting technique with a stoichiometric ratio of pure elements La(3N), Pd(4N), Ni(4N), Ge(5N), and Si(5N) in an Ar gas atmosphere. The details are described in [19, 21, 22]. The arc-melted buttons were annealed at 900–1100 °C in a vacuum, typically for 1 week. The x-ray diffraction patterns of  $La_3Pd_4Ge_4$ ,  $La_3Ni_4Si_4$ , and  $La_3Ni_4Ge_4$  show that their crystal structure is identical to the  $U_3Ni_4Si_4$ -type, with a tiny fraction of impurity phases mainly attributed to the  $ThCr_2Si_2$ -type component. The fraction of the impurities in  $La_3Pd_4Ge_4$ ,  $La_3Ni_4Si_4$ , and  $La_3Ni_4Ge_4$  is less than a few per cent. Meanwhile, for  $La_3Pd_4Si_4$ , it is found to be above 10%, which led us to exclude this compound

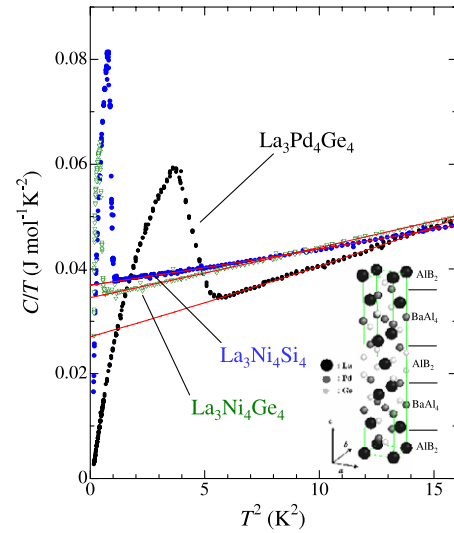


**Figure 1.** Total specific heat in  $La_3Pd_4Ge_4$ ,  $La_3Ni_4Si_4$ , and  $La_3Ni_4Ge_4$  plotted in  $C/T$  versus  $T^2$ . The inset shows the basic  $U_3Ni_4Si_4$ -type structure of  $La_3Pd_4Ge_4$ . Solid lines show fits to the data by  $C = \gamma_n T + \beta T^3 + \delta T^5$ . The parameters  $\gamma_n$ ,  $\beta$ ,  $\delta$  in these superconductors are summarized in table 1.

from the present study. The  $ThCr_2Si_2$ -type compounds of  $LaPd_2Ge_2$ ,  $LaNi_2Si_2$ , and  $LaNi_2Ge_2$  were also synthesized by arc-melting. Single phased samples were obtained for these compounds. Specific heat measurements by the thermal relaxation method were performed in a temperature range from 0.4 to 5.0 K on samples with masses of about 13–28 mg. A platelet shaped polycrystal with polished surfaces is cut from the annealed button, and mounted on a small sapphire chip on which a serpentine metallic heater is evaporated. A Cernox temperature sensor attached to the sapphire chip with gold leads is used to measure the heat capacity. In our system, the level of addenda is 14.0 nJ K<sup>-1</sup> at 1 K and 0.6 μJ K<sup>-1</sup> at 5 K, which is independent of the applied field up to 5 T. Precise measurements on the specific heat are carried out by fitting the addenda polynomially and subtracting them.

## 3. Results and discussion

The main panel of figure 1 shows a plot of specific heat divided by temperature,  $C/T$ , in  $La_3Pd_4Ge_4$ ,  $La_3Ni_4Si_4$ , and  $La_3Ni_4Ge_4$  as a function of  $T^2$ , with the inset showing the basic  $U_3Ni_4Si_4$ -type crystal structure of  $La_3Pd_4Ge_4$ . Clear specific heat jumps appear in all the samples at temperatures agreeing with the transport data for zero resistivity. The normal state specific heat in each compound is fitted by a linear combination of the electronic contribution  $C_{el} = \gamma_n T$  and the phonon part  $C_{ph} = \beta T^3 + \delta T^5$ , as drawn by the solid lines. The parameters  $\gamma_n$ ,  $\beta$ , and  $\delta$ , obtained from the data are summarized in table 1. Here,  $\gamma_n = 27.0$  mJ mol<sup>-1</sup> K<sup>-2</sup> for  $La_3Pd_4Ge_4$ , 36.9 mJ mol<sup>-1</sup> K<sup>-2</sup> for  $La_3Ni_4Si_4$ , and 34.5 mJ mol<sup>-1</sup> K<sup>-2</sup> for  $La_3Ni_4Ge_4$ , respectively, are obtained.  $La_3Pd_4Ge_4$  shows a large  $\delta T^5$  term, suggesting a contribution from complex phonon densities of states. From the relationship  $\beta = (12\pi^4/5)Nk_B(1/\Theta_D)^3$ , the Debye temperature,  $\Theta_D$ , is

**Table 1.** The normal and superconducting parameters of  $U_3Ni_4Si_4$ -type  $La_3Pd_4Ge_4$ ,  $La_3Ni_4Si_4$ ,  $La_3Ni_4Ge_4$ , and  $ThCr_2Si_2$ -type  $LaPd_2Ge_2$ ,  $LaNi_2Si_2$ ,  $LaNi_2Ge_2$  derived from the specific heat results.

	$T_c^{on}$ (K)	$T_c^{th}$ (K)	$\gamma_n$ (mJ mol <sup>-1</sup> K <sup>-2</sup> )	$\beta$ (mJ mol <sup>-1</sup> K <sup>-4</sup> )	$\delta$ ( $\mu$ J mol <sup>-1</sup> K <sup>-6</sup> )	$\Theta_D$ (K)
$La_3Pd_4Ge_4$	2.50	2.23	27.0	1.27	12.7	256
$La_3Ni_4Si_4$	1.00	0.96	36.9	0.645	4.40	321
$La_3Ni_4Ge_4$	0.76	0.74	34.5	0.930	2.76	284
$LaPd_2Ge_2$	1.10	0.96	8.26	0.393	5.05	291
$LaNi_2Si_2$	—	—	11.3	0.208	1.97	360
$LaNi_2Ge_2$	—	—	14.5	0.273	3.14	328
	$\lambda_{ph}$	$N(E_F)$ (states/eV fu)	$2\Delta_0^{exp}/k_B T_c^{th}$	$\Delta_0^{exp}$ (meV)	$\Delta_0^{BCS}$ (meV)	$\Delta C/\gamma_n T_c^{th}$
$La_3Pd_4Ge_4$	0.48–0.55	3.86–3.69	3.08	0.30	0.34	1.24
$La_3Ni_4Si_4$	0.39–0.43	5.43–5.32	3.26	0.14	0.16	1.32
$La_3Ni_4Ge_4$	0.38–0.43	5.16–4.97	2.83	0.09	0.12	0.95
$LaPd_2Ge_2$	0.39–0.45	1.69–1.63	3.65	0.15	0.15	1.05
$LaNi_2Si_2$	( $\lambda_{ph} < 0.33$ –0.38)	(2.33)	—	—	—	—
$LaNi_2Ge_2$	( $\lambda_{ph} < 0.33$ –0.38)	(2.99)	—	—	—	—

estimated as 256 K for  $La_3Pd_4Ge_4$ , 321 K for  $La_3Ni_4Si_4$ , and 284 K for  $La_3Ni_4Ge_4$ . The electron–phonon coupling constant,  $\lambda_{ph}$ , is calculated by the McMillan formula:

$$T_c = \frac{\Theta_D}{1.45} \exp \left[ -\frac{1.04(1 + \lambda_{ph})}{\lambda_{ph} - \mu^*(1 + 0.62\lambda_{ph})} \right], \quad (1)$$

where  $\mu^*$  is the Coulomb pseudopotential [23]. Taking a typical value of  $\mu^* = 0.10$ –0.13 for metallic materials [23], we obtain  $\lambda_{ph} = 0.48$ –0.55 for  $La_3Pd_4Ge_4$ , 0.39–0.43 for  $La_3Ni_4Si_4$ , and 0.38–0.45 for  $La_3Ni_4Ge_4$ . The electronic density of states at the Fermi level,  $N(E_F)$ , is given by the relationship [23]

$$\gamma_n = \frac{2}{3}\pi^2 k_B^2 (1 + \lambda_{ph}) N(E_F). \quad (2)$$

For the values of  $\gamma_n$  and  $\lambda_{ph}$  derived above,  $N(E_F) = 3.86$ –3.69 states/(eV fu) is calculated for  $La_3Pd_4Ge_4$ .  $N(E_F) = 5.43$ –5.32 and 5.16–4.97 states/(eV fu) are derived for  $La_3Ni_4Si_4$  and  $La_3Ni_4Ge_4$ , respectively.

The electronic specific heat,  $C_{el} = C - \beta T^3 - \delta T^5$ , in the three  $U_3Ni_4Si_4$ -type superconductors is shown in figure 2. The main panel shows a plot of  $C_{el}$  versus  $T$ , and the inset has a plot of  $C_{el}/\gamma_n T$  versus  $T/T_c^{th}$ , respectively. Here,  $T_c^{th}$  denotes the thermodynamic critical temperature considering the entropy balance. As drawn by the solid lines,  $C_{el}$  is fitted by a thermally excited exponential behavior,  $C_{el} \sim \exp(-\Delta_0/k_B T)$ , expected for the BCS superconductivity. The superconducting gap,  $\Delta_0^{exp}$ , determined by the experiments is 0.30 meV for  $La_3Pd_4Ge_4$ , 0.14 meV for  $La_3Ni_4Si_4$ , and 0.09 meV for  $La_3Ni_4Ge_4$ . These values are slightly smaller than the theoretical BCS values of  $\Delta_0^{BCS} = 0.33$ , 0.16 and 0.12 meV for  $La_3Pd_4Ge_4$ ,  $La_3Ni_4Si_4$ , and  $La_3Ni_4Ge_4$ , expected for the  $T_c^{th} \sim 2.23$ , 0.96, and 0.74 K, respectively. For  $La_3Pd_4Ge_4$ , the gap  $\Delta_0^{exp}$  gives a value  $2\Delta_0^{exp}/k_B T_c^{th} \sim 3.08$ . The electronic specific heat jump at  $T_c^{th}$  brings  $\Delta C_{el}/\gamma_n T_c^{th} \sim 1.24$ . For  $La_3Ni_4Si_4$ ,  $2\Delta_0^{exp}/k_B T_c^{th} \sim 3.26$  and  $\Delta C_{el}/\gamma_n T_c^{th} \sim 1.32$  are obtained. These are slightly smaller, but comparable with the BCS values of  $2\Delta_0^{BCS}/k_B T_c^{th} = 3.53$  and  $\Delta C_{el}/\gamma_n T_c^{th} = 1.43$ . Apart from the above two compounds,  $La_3Ni_4Ge_4$  shows smaller values

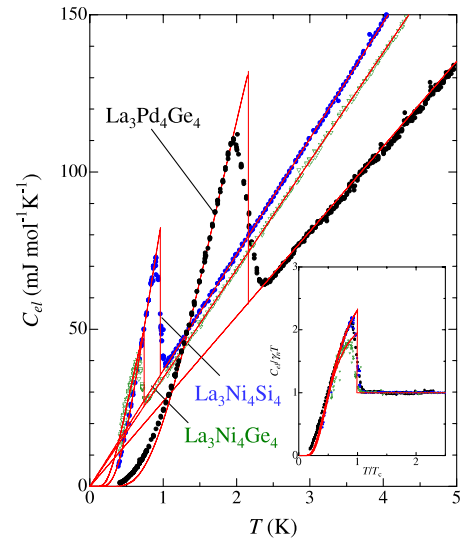


**Figure 2.** Electronic specific heat,  $C_{el}$ , in  $La_3Pd_4Ge_4$ ,  $La_3Ni_4Si_4$ , and  $La_3Ni_4Ge_4$ . The inset shows normalized plots in  $C_{el}/\gamma_n T$  versus  $T/T_c^{th}$ . All the data are fitted by the BCS exponential behavior as shown by the solid lines.

as  $2\Delta_0^{exp}/k_B T_c^{th} \sim 2.83$  and  $\Delta C_{el}/\gamma_n T_c^{th} \sim 0.95$ . Typically, such a small jump at  $T_c$  is observed when the sample includes impurities. However, we have checked that the fraction of impurities in our sample is less than a few per cent and cannot explain the small size of the jump height ( $\sim 30\%$  smaller than the BCS value). Growth of single crystalline samples and experiments using them are highly recommended to develop this work further.

For  $La_3Pd_4Ge_4$ , the magnetic field dependence of the Sommerfeld coefficient,  $\gamma_s(H)$ , is also investigated. Figure 3 shows a plot of  $\gamma_s(H)$  versus  $\mu_0 H$  in  $La_3Pd_4Ge_4$  derived from the field evolution of the specific heat (the inset). The value of  $\gamma_s(H)$  is determined by extrapolating the  $C/T$  versus  $T^2$  curves at  $T^2 \leq 0.5$  K<sup>2</sup> with the equation  $C/T = \gamma_s + \beta_s T^2$ . The field dependence of  $\gamma_s(H)$  in  $La_3Pd_4Ge_4$  is well fitted by the relationship  $\gamma_s(H) = \gamma_s(0) + \gamma_n H/H_{c2}$ , which is in marked contrast to the behavior  $\gamma_s(H) = \gamma_s(0) + \gamma_n (H/H_{c2})^{1/2}$  at

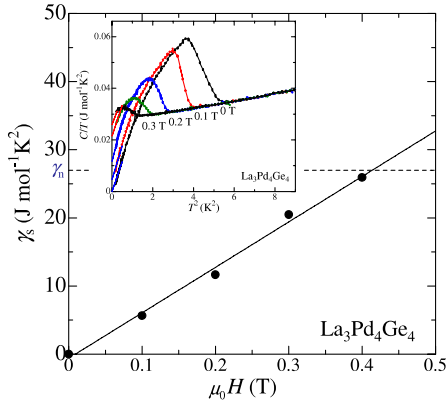


**Figure 3.** Magnetic field dependence of the Sommerfeld coefficient in the superconducting state,  $\gamma_s(H)$ , defined by extrapolating the  $C/T$  versus  $T^2$  plot (the inset) at  $T^2 \leq 0.5 \text{ K}^2$ . The solid line shows the function  $\gamma_s(H) = \gamma_s(0) + \gamma_n H/H_{c2}$ . The field dependence of  $\gamma_s(H)$  is in good agreement with the conventional BCS superconductor with an isotropic gap.

$H \ll H_{c2}$ , expected for nodal superconductors [8, 24]. As well as the exponential behavior of the  $C_{el}$  in figure 2,  $\gamma_s(H) \propto H$  shows that  $\text{La}_3\text{Pd}_4\text{Ge}_4$  is a fully gapped superconductor, in which  $\gamma_s(H)$  is proportional to the density of vortices, carrying a zero energy density of states. It should also be noted that the value of  $\mu_0 H_{c2} \sim 0.4 \text{ T}$  is in good agreement with our earlier results determined by the linear extrapolation of the  $H_{c2}(T)$  curve obtained from magnetization measurements [19]. In addition, the validity of the present experiments is also confirmed by deducing the thermodynamic critical field,  $\mu_0 H_c$ , from the specific heat data. According to the BCS prediction, the zero temperature value of the thermodynamic critical field,  $\mu_0 H_c(0)$ , is given by the following relationship:

$$\mu_0 V_m H_c(0)^2 = 0.47 \gamma_n T_c^2 \quad (3)$$

where  $V_m$  represents the molar volume. By taking the lattice parameters  $a = 4.2293(1) \text{ \AA}$ ,  $b = 4.3823(1) \text{ \AA}$ , and  $c = 25.0109(8) \text{ \AA}$  [20] as well as the derived values of  $\gamma_n$  and  $T_c$ ,  $\mu_0 H_c(0) = 23.8 \text{ mT}$  is obtained. This is close to the value of  $\mu_0 H_c(0) = 28 \text{ mT}$  [19] derived from  $\mu_0 H_c(0) = \mu_0 H_{c2}^{\text{WHH}}(0)/\sqrt{2}\kappa(0)$ , where  $\kappa(0)$  denotes the Ginsburg–Landau parameter and  $H_{c2}^{\text{WHH}}(0) = -0.69T_c(dH_{c2}/dT)_{T_c}$ , the upper critical field defined by the Werthamer–Helfand–Hohemberg (WHH) formula [25, 26].

According to the past works, all the  $\text{U}_3\text{Ni}_4\text{Si}_4$ -type superconductors based on lanthanum exhibit higher  $T_c$ s than the related compounds having the  $\text{ThCr}_2\text{Si}_2$ -type structure, i.e.  $\text{LaPd}_2\text{Ge}_2$ ,  $\text{LaPd}_2\text{Si}_2$ ,  $\text{LaNi}_2\text{Ge}_2$ , and  $\text{LaNi}_2\text{Si}_2$  with  $T_c \sim 1.17, 0.39 \text{ K}$  for the two former compounds and no superconductivity in the latter two [4, 27]. Owing to the relatively higher  $T_c$  of  $\text{U}_3\text{Ni}_4\text{Si}_4$ -type superconductors, we also studied the thermodynamic properties in  $\text{LaPd}_2\text{Ge}_2$ ,  $\text{LaNi}_2\text{Si}_2$  and  $\text{LaNi}_2\text{Ge}_2$  as reference compounds, which are considered as the segments of  $\text{La}_3\text{Pd}_4\text{Ge}_4$ ,  $\text{La}_3\text{Ni}_4\text{Si}_4$ ,  $\text{La}_3\text{Ni}_4\text{Ge}_4$ .

Figure 4 shows a plot of  $C/T$  versus  $T^2$  in  $\text{LaPd}_2\text{Ge}_2$ ,  $\text{LaNi}_2\text{Si}_2$ , and  $\text{LaNi}_2\text{Ge}_2$ . In  $\text{LaNi}_2\text{Si}_2$  and  $\text{LaNi}_2\text{Ge}_2$ ,  $C/T$ – $T^2$  curves show up-turns at low temperatures, which are fitted

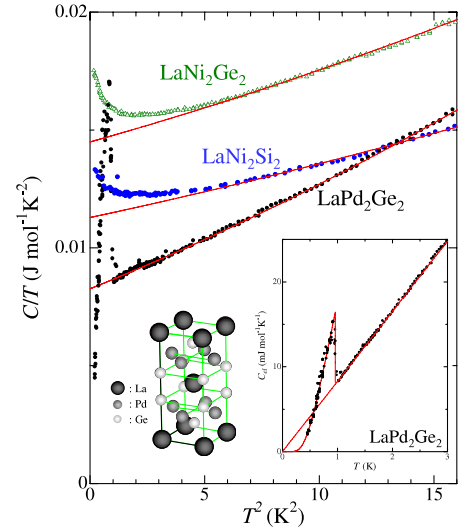


**Figure 4.** Specific heat of  $\text{ThCr}_2\text{Si}_2$ -type  $\text{LaPd}_2\text{Ge}_2$ ,  $\text{LaNi}_2\text{Si}_2$ , and  $\text{LaNi}_2\text{Ge}_2$  plotted in  $C/T$  versus  $T^2$ . The right inset shows the electronic specific heat in  $C_{el}$  versus  $T$ . The basic crystal structure of  $\text{LaPd}_2\text{Ge}_2$  is shown in the left inset.

by the Schottky-type anomaly for a two-level system with energy difference  $\delta \sim 1.18 \text{ K}$ , presumably arising from the crystalline electric field splitting of the Ni d-electron orbital. Following the same analysis on the normal state specific heat,  $\gamma_n = 8.26 \text{ mJ mol}^{-1} \text{ K}^{-2}$ ,  $\beta = 0.393 \text{ mJ mol}^{-1} \text{ K}^{-4}$ , and  $\delta = 5.06 \text{ \mu J mol}^{-1} \text{ K}^{-6}$  are derived for  $\text{LaPd}_2\text{Ge}_2$ . On the other hand, by fitting the data at  $T > 2.5 \text{ K}$ ,  $\gamma = 11.3 \text{ mJ mol}^{-1} \text{ K}^{-2}$ ,  $\beta = 0.208 \text{ mJ mol}^{-1} \text{ K}^{-4}$ ,  $\delta = 1.97 \text{ \mu J mol}^{-1} \text{ K}^{-6}$  and  $\gamma = 14.5 \text{ mJ mol}^{-1} \text{ K}^{-2}$ ,  $\beta = 0.273 \text{ mJ mol}^{-1} \text{ K}^{-4}$ ,  $\delta = 3.14 \text{ \mu J mol}^{-1} \text{ K}^{-6}$  are obtained for  $\text{LaNi}_2\text{Si}_2$  and  $\text{LaNi}_2\text{Ge}_2$ , respectively.  $\Theta_D$  is calculated as 291 K for  $\text{LaPd}_2\text{Ge}_2$ , 360 K for  $\text{LaNi}_2\text{Si}_2$ , and 328 K for  $\text{LaNi}_2\text{Ge}_2$ . The electron–phonon coupling constant in  $\text{LaPd}_2\text{Ge}_2$  is calculated as  $\lambda_{ph} = 0.39$ – $0.45$  for  $\mu^* = 0.10$ – $0.13$ . For  $\text{LaNi}_2\text{Si}_2$  and  $\text{LaNi}_2\text{Ge}_2$ , the absence of superconductivity, at least down to 320 mK, suggests  $\lambda_{ph} < 0.33$ – $0.38$  in these compounds.  $N(E_F)$  in  $\text{LaPd}_2\text{Ge}_2$  is derived as 1.69–1.63 states/(eV fu) for the values  $\gamma_n = 8.26 \text{ mJ mol}^{-1} \text{ K}^{-2}$  and  $\lambda_{ph} = 0.39$ – $0.45$ . On the other hand,  $N(E_F) = 2.33$  and 2.99 states/(eV fu) are given for  $\text{LaNi}_2\text{Si}_2$  and  $\text{LaNi}_2\text{Ge}_2$  in the limit of  $\lambda_{ph} \rightarrow 0$ . The electronic specific heat,  $C_{el}$ , for  $\text{LaPd}_2\text{Ge}_2$  is analyzed in the inset of figure 4. In the superconducting state of  $\text{LaPd}_2\text{Ge}_2$ ,  $C_{el}$  is fitted by the BCS model, yielding values of  $\Delta C_{el}/\gamma_n T_c^{\text{th}} \sim 1.05$  and  $\Delta_0^{\text{exp}} \sim 0.15 \text{ meV}$  with  $2\Delta_0^{\text{exp}}/k_B T_c^{\text{th}} \sim 3.65$ .

In the following, we compare the thermodynamic and superconducting properties of  $\text{La}_3\text{Pd}_4\text{Ge}_4$ ,  $\text{La}_3\text{Ni}_4\text{Si}_4$ , and  $\text{La}_3\text{Ni}_4\text{Ge}_4$ , and also  $\text{LaPd}_2\text{Ge}_2$ ,  $\text{LaNi}_2\text{Ge}_2$ , and  $\text{LaNi}_2\text{Si}_2$ . All the parameters obtained in the present experiments are summarized in table 1. According to the simple BCS model, a high electronic density of states at the Fermi level, Debye temperature, and strong electron–phonon coupling will bring higher  $T_c$ , as it is given as  $T_c = 1.33\Theta_D \exp[-1/N(E_F)V]$ , where  $V$  is the strength of the electron–phonon interaction. Looking over the other  $\text{ThCr}_2\text{Si}_2$ -type derivatives, quaternary

borocarbides  $\text{RNi}_2\text{B}_2\text{C}$  ( $\text{R} = \text{rare earth}$ ) show fairly high  $T_c$ s [9]. The high  $T_c$ s of  $\text{RNi}_2\text{B}_2\text{C}$  are believed to come from a moderately strong electron–phonon coupling, together with a large value of  $N(E_F)$  contributed by the Ni 3d band. Getting back to the present three  $\text{U}_3\text{Ni}_4\text{Si}_4$ -type superconductors,  $\text{La}_3\text{Ni}_4\text{Si}_4$  shows the highest values in  $\Theta_D$ ,  $\gamma_n$ , and  $N(E_F)$ . Similar values of  $\gamma_n$  and  $N(E_F)$  are found in  $\text{La}_3\text{Ni}_4\text{Ge}_4$ . On the other hand,  $\text{La}_3\text{Pd}_4\text{Ge}_4$  shows the lowest. The relatively larger  $\gamma_n$  and  $N(E_F)$  in  $\text{La}_3\text{Ni}_4\text{Si}_4$  and  $\text{La}_3\text{Ni}_4\text{Ge}_4$  are considered to originate from the Ni 3d band. However, in spite of larger values of  $N(E_F)$  in  $\text{La}_3\text{Ni}_4\text{Si}_4$  and  $\text{La}_3\text{Ni}_4\text{Ge}_4$ ,  $T_c$  values in these compounds are less than half of those in  $\text{La}_3\text{Pd}_4\text{Ge}_4$ . Judging from the present analyses based on the specific heat measurements, the difference in the  $T_c$ s in  $\text{La}_3\text{Pd}_4\text{Ge}_4$ ,  $\text{La}_3\text{Ni}_4\text{Ge}_4$ , and  $\text{La}_3\text{Ni}_4\text{Si}_4$  is attributed to the strength of the electron–phonon coupling. In contrast to the smaller values of  $\gamma_n$ ,  $N(E_F)$ , and  $\Theta_D$ ,  $\text{La}_3\text{Pd}_4\text{Ge}_4$  has about 20% larger  $\lambda_{\text{ph}}$  than the other  $\text{U}_3\text{Ni}_4\text{Si}_4$ -type superconductors. It should also be noted that such a trend of the electron–phonon coupling is also found in the  $\text{ThCr}_2\text{Si}_2$ -type compounds. Looking at the parameters in  $\text{LaPd}_2\text{Ge}_2$ ,  $\text{LaNi}_2\text{Si}_2$ , and  $\text{LaNi}_2\text{Ge}_2$  again,  $\Theta_D$  and  $N(E_F)$  appear to have less weight on the  $T_c$ s in these compounds. Instead,  $\lambda_{\text{ph}} = 0.39\text{--}0.45$  for  $\text{LaPd}_2\text{Ge}_2$ , together with  $\lambda_{\text{ph}} < 0.33\text{--}0.38$  for  $\text{LaNi}_2\text{Si}_2$  and  $\text{LaNi}_2\text{Ge}_2$ , suggesting that the differences in  $T_c$  in the three  $\text{ThCr}_2\text{Si}_2$ -type compounds are mainly due to differences in  $\lambda_{\text{ph}}$ . Moreover, differences in  $\lambda_{\text{ph}}$  are also found between the  $\text{U}_3\text{Ni}_4\text{Si}_4$ - and  $\text{ThCr}_2\text{Si}_2$ -type compounds. Our thermodynamic investigations show that all the  $\text{U}_3\text{Ni}_4\text{Si}_4$ -type superconductors based on lanthanum have larger  $\lambda_{\text{ph}}$  than the  $\text{ThCr}_2\text{Si}_2$ -type compounds, while  $T_c$  is less dependent on  $\Theta_D$  or  $N(E_F)$ . In figure 5, the relationship between  $T_c^{\text{th}}$  and  $\lambda_{\text{ph}}$  (derived for  $\mu^* = 0.13$ ) in the  $\text{U}_3\text{Ni}_4\text{Si}_4$ - and the  $\text{ThCr}_2\text{Si}_2$ -type compounds are summarized. Black closed circles are the data from the specific heat results. For  $\text{LaNi}_2\text{Si}_2$  and  $\text{LaNi}_2\text{Ge}_2$ , an indistinct spot at  $\lambda_{\text{ph}} \leq 0.38$  shows the expected positions of  $T_c^{\text{th}}$  versus  $\lambda_{\text{ph}}$ , if these compounds show superconductivity below 320 mK. On the other hand, those for  $\text{La}_3\text{Pd}_4\text{Si}_4$  and  $\text{LaPd}_2\text{Si}_2$  are deduced by considering the  $T_c$ s of these compounds.  $T_c^{\text{th}}$ s in the  $\text{U}_3\text{Ni}_4\text{Si}_4$ - and  $\text{ThCr}_2\text{Si}_2$ -type compounds appear to be universally dependent on  $\lambda_{\text{ph}}$ . For a more elaborate understanding, the role of the electron–phonon coupling investigated by the present thermodynamic measurements should be confirmed by other experimental techniques such as Raman spectroscopy, etc. Detailed band structure calculations are also needed.

Finally, let us comment on a potential of the intermetallic compounds crystallized in the  $\text{U}_3\text{Ni}_4\text{Si}_4$ -type structure. Concerning the nature of the gap symmetry, the present experiments revealed that  $\text{La}_3\text{Pd}_4\text{Ge}_4$ ,  $\text{La}_3\text{Ni}_4\text{Si}_4$ ,  $\text{La}_3\text{Ni}_4\text{Ge}_4$ , and  $\text{LaPd}_2\text{Ge}_2$  are all of the conventional BCS-type. This is rationalized considering the fact that lanthanum does not have 4f electrons and no hybridization occurs between the conduction electrons. If the lanthanum in the  $\text{U}_3\text{Ni}_4\text{Si}_4$ -type structure can be substituted for the other rare-earths, it may bring some exotic properties to the superconducting state, as have been investigated in a number of  $\text{ThCr}_2\text{Si}_2$  derivatives. So far, most of the rare-earth substitutions

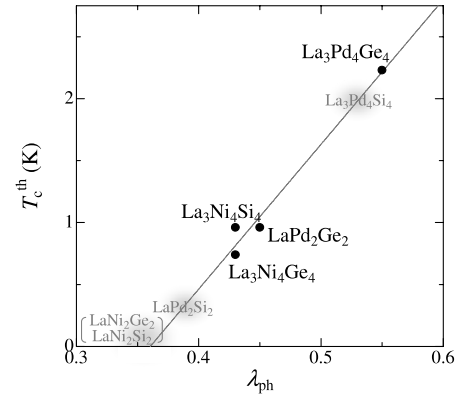


**Figure 5.** A plot of  $T_c^{\text{th}}$  versus  $\lambda_{\text{ph}}$  (derived for  $\mu^* = 0.13$ ) in  $\text{U}_3\text{Ni}_4\text{Si}_4$ - and  $\text{ThCr}_2\text{Si}_2$ -type compounds. The black closed circles are data for  $\text{La}_3\text{Pd}_4\text{Ge}_4$ ,  $\text{La}_3\text{Ni}_4\text{Si}_4$ ,  $\text{La}_3\text{Ni}_4\text{Ge}_4$ , and  $\text{LaPd}_2\text{Ge}_2$ . The indistinct spot for  $\text{LaNi}_2\text{Ge}_2$ ,  $\text{LaNi}_2\text{Si}_2$ , and also  $\text{LaPd}_2\text{Si}_2$ ,  $\text{La}_3\text{Pd}_4\text{Si}_4$  suggests the expected positions of  $T_c$  versus  $\lambda_{\text{ph}}$  deduced from the present study.

are reported to fail to stabilize the  $\text{U}_3\text{Ni}_4\text{Si}_4$ -type structure. Alternatively, compounds with  $\text{Gd}_3\text{Cu}_4\text{Ge}_4$ -type structure, such as  $\text{Ln}_3\text{Pd}_4\text{Ge}_4$  ( $\text{Ln} = \text{Y, Gd, Tb, Dy, Ho, Er, Tm, and Yb}$ ) [28–33] are synthesized. In these compounds, cages of Pd–Ge are formed instead of the Pd–Ge networks in  $\text{La}_3\text{Pd}_4\text{Ge}_4$ . By contrast, substitution of the lanthanum by cerium is reported to succeed in synthesizing  $\text{Ce}_3\text{Pd}_4\text{Ge}_4$ , crystallizing in the  $\text{U}_3\text{Ni}_4\text{Si}_4$ -type structure with Kondo lattice properties [14]. Since these  $\text{U}_3\text{Ni}_4\text{Si}_4$ - and  $\text{Gd}_3\text{Cu}_4\text{Ge}_4$ -type compounds are candidates for the various ground states governed by competition between the RKKY and Kondo interactions, more investigation is urgently needed on the possibility of novel phenomena related to the superconductivity and magnetism. Single crystal growth of  $\text{U}_3\text{Ni}_4\text{Si}_4$ -type compounds will also open up a new area for investigations.

#### 4. Summary

To summarize, we have presented a systematic investigation on the thermodynamic properties in ternary  $\text{U}_3\text{Ni}_4\text{Si}_4$ -type intermetallic superconductors  $\text{La}_3\text{Pd}_4\text{Ge}_4$ ,  $\text{La}_3\text{Ni}_4\text{Si}_4$ , and  $\text{La}_3\text{Ni}_4\text{Ge}_4$ , and  $\text{ThCr}_2\text{Si}_2$ -type  $\text{LaPd}_2\text{Ge}_2$ ,  $\text{LaNi}_2\text{Si}_2$ , and  $\text{LaNi}_2\text{Ge}_2$ . From the normal state specific heat, the Sommerfeld coefficient,  $\gamma_n$ , the Debye temperature,  $\Theta_D$ , and the electronic density of states at the Fermi level,  $N(E_F)$ , are estimated. The electronic specific heat in each of these compounds showed thermally excited exponential behavior in the superconducting state. In  $\text{La}_3\text{Pd}_4\text{Ge}_4$ , the Sommerfeld coefficient in the superconducting state,  $\gamma_s$ , showed linear field dependence. These results suggest that  $\text{La}_3\text{Pd}_4\text{Ge}_4$ ,  $\text{La}_3\text{Ni}_4\text{Si}_4$ ,  $\text{La}_3\text{Ni}_4\text{Ge}_4$ , and  $\text{LaPd}_2\text{Ge}_2$  are superconductors with isotropic gaps. Although,  $\text{La}_3\text{Ni}_4\text{Si}_4$  and  $\text{La}_3\text{Ni}_4\text{Ge}_4$  show higher  $N(E_F)$  than  $\text{La}_3\text{Pd}_4\text{Ge}_4$ , presumably contributed by the Ni 3d band, their  $T_c$ s are lower than that of  $\text{La}_3\text{Pd}_4\text{Ge}_4$ . The present investigations on the specific heat suggest that this is due to differences in the electron–phonon coupling. The electron–phonon coupling constant,  $\lambda_{\text{ph}}$ , in  $\text{La}_3\text{Pd}_4\text{Ge}_4$

is larger than those in  $\text{La}_3\text{Ni}_4\text{Si}_4$  and  $\text{La}_3\text{Ni}_4\text{Ge}_4$ . The same relationship was found for  $\text{ThCr}_2\text{Si}_2$ -type  $\text{LaPd}_2\text{Ge}_2$ ,  $\text{LaNi}_2\text{Si}_2$ , and  $\text{LaNi}_2\text{Ge}_2$ . Additionally, the  $\text{U}_3\text{Ni}_4\text{Si}_4$ -type  $\text{La}_3\text{Pd}_4\text{Ge}_4$ ,  $\text{La}_3\text{Ni}_4\text{Si}_4$ , and  $\text{La}_3\text{Ni}_4\text{Ge}_4$  showed higher  $\lambda_{\text{ph}}$  than the corresponding  $\text{ThCr}_2\text{Si}_2$ -type  $\text{LaPd}_2\text{Ge}_2$ ,  $\text{LaNi}_2\text{Si}_2$ , and  $\text{LaNi}_2\text{Ge}_2$ . The role of the electron–phonon coupling investigated with the present thermodynamic measurements should also be confirmed using other experimental techniques.

## Acknowledgments

The authors thank Dr I Hase at AIST and Dr M Imai at NIMS for fruitful discussions. SK is supported by a Grant-in-Aid Scientific Research for Young Scientists (B), from the Ministry of Education, Culture, Sports, Science and Technology (MEXT), Japan.

## References

- [1] Ban Z and Sikirica M 1965 *Acta Crystallogr.* **18** 594
- [2] Just G and Pauffer P 1996 *J. Alloys Compounds* **232** 1
- [3] Steglich F, Aarts J, Bredl C D, Lieke W, Meschede D, Franz W and Schafer H 1979 *Phys. Rev. Lett.* **43** 1892
- [4] Hull G W, Wernick J H, Geballe T H, Waszczak J V and Bernardini J E 1981 *Phys. Rev. B* **24** 6715
- [5] Cava R J, Takagi H, Batlogg B, Zandbergen H W, Krajewski J J, Peck W F Jr, van Dover R B, Felder R J, Siegrist T, Mizuhashi K, Lee J O, Eisaki H, Carter S A and Uchida S 1994 *Nature* **367** 146
- [6] Cava R J, Takagi H, Zandbergen H W, Krajewski J J, Peck W F Jr, Siegrist T, Batlogg B, van Dover R B, Felder R J, Mizuhashi K, Lee J O, Eisaki H and Uchida S 1994 *Nature* **367** 252
- [7] Cava R J, Batlogg B, Siegrist T, Krajewski J J, Peck W F Jr, Carter S, Felder R J, Takagi H and van Dover R B 1994 *Phys. Rev. B* **49** 12384
- [8] Nohara M, Isshiki M, Takagi H and Cava R J 1997 *J. Phys. Soc. Japan* **66** 1888
- [9] Muller K H and Narozhnyi V N 2001 *Rep. Prog. Phys.* **64** 943
- [10] Yarmolyuk J P, Akselrud J G, Grin Yu N, Fundamenskii V S and Gladyshevskii E I 1979 *Sov. Phys.—Crystallogr.* **24** 332
- [11] Hovestreydt E, Kliipp K and Parthe E 1982 *Acta Crystallogr. B* **38** 1803
- [12] Parthe E, Chabot B, Braun H F and Engel N 1983 *Acta Crystallogr. B* **39** 588
- [13] Rogl P, Chevalier B and Etourneau J 1990 *J. Solid State Chem.* **88** 429
- [14] Im H J, Kwona Y S and Jung M H 2002 *Solid State Commun.* **124** 181
- [15] Chevalier B and Etourneau J 1999 *J. Magn. Magn. Mater.* **196/197** 880
- [16] Kuang J P, Cui H J, Li J Y, Yang F M, Nakotte H, Briick E and de Boer F R 1992 *J. Magn. Magn. Mater.* **104** 1475
- [17] Kaczorowski D, Noel H and Potel M 1995 *Physica B* **206/207** 457
- [18] Pechev S, Chevalier B, Laargue D, Darriet B, Roisnel T and Etourneau J 1999 *J. Magn. Magn. Mater.* **191** 282
- [19] Fujii H, Mochiku T, Takeya H and Sato A 2005 *Phys. Rev. B* **72** 214520
- [20] Mochiku T, Fujii H, Takeya H, Wuernisha T, Mori K, Ishigaki T, Kamiyama T and Hirata K 2007 *Physica C* **463–465** 182
- [21] Fujii H 2006 *J. Phys.: Condens. Matter* **18** 8037
- [22] Fujii H and Kasahara S 2008 *J. Phys.: Condens. Matter* **20** 075202
- [23] McMillan W L 1968 *Phys. Rev.* **167** 331
- [24] Volovik G E 1993 *JETP Lett.* **58** 469
- [25] Helfand E and Werthamer W R 1966 *Phys. Rev.* **147** 288
- [26] Werthamer N R, Helfand E and Hohemberg P C 1966 *Phys. Rev.* **147** 295
- [27] Palstra T T M, Lu G, Menovsky A A, Nieuwenhuys G J, Kes P H and Mydosh J A 1986 *Phys. Rev. B* **34** 4566
- [28] Rieger W 1970 *Monatsch. Chem.* **101** 449
- [29] Liebrich O, Schafer H and Weiss A 1970 *Z. Naturf. b* **25** 650
- [30] Gladyshevskii R E, Sologub O L and Parthe E 1991 *J. Alloys Compounds* **176** 329
- [31] Prots' Yu M, Bodak O I, Pecharsky V K, Salamakha P S and Seropegin Yu D 1993 *Z. Kristallogr.* **205** 331
- [32] Salamakha P, Sologub O, Yakinthos J K and Routsis Ch D 1998 *J. Alloys Compounds* **267** 192
- [33] Niepmann D, Prots' Y M, Pottgen R and Jeitschko W 2000 *J. Solid State Chem.* **154** 329